JOURNAL OF THEORETICAL
AND APPLIED MECHANICS
51, 2, pp. 363-373, Warsaw 2013

STUDY OF TOPOLOGY AND VORTEX STRUCTURE IN TURBINE CASCADES WITH TIP CLEARANCE UNDER DIFFERENT INCIDENCE ANGLES

Pei-Gang Yan

Harbin Institute of Technology, School of Energy Science and Engineering, Harbin, China

Xiao-Qing Qiang, Jin-Fang Teng

Shanghai Jiao Tong University, School of Aeronautics and Astronautics, Shanghai, China

e-mail: qiangxiaoqing@sjtu.edu.cn

Wan-Jin Han

Harbin Institute of Technology, School of Energy Science and Engineering, Harbin, China

Three sets of conventional straight, positive curved and negative curved turbine cascades with tip clearance were tested with experimental measurement. The impact of incidence angles and blade bending on the tip leakage was studied under larger clearance (0.036 of span). An ink trace visualization of the wall flow and topology theory was adopted and thus the topological structures of the blade surface, the upper and lower end wall were analyzed in this paper. It was found that, compared with the same cascade under the zero incidence angle, the saddle points all move to the upstream, the scope of the separation expands along the flow and span direction, and the separation line of the upper and lower passage vortex climb to the middle span of the blade when the flow incidence angle increased from zero to 20°. Under the condition of zero and 20° incidence angle, the positive curved blade will eliminate the upper passage vortex. The numbers of singular points are reduced and the interaction loss between the passage vortex and the leakage vortex is greatly reduced too. On the other hand, it also strengthens the blocking effect of the end wall cross flow on the leakage flow, thereby reduces the relative leakage flow rate.

Key words: turbine cascade, tip clearance, topological rules, experimental study

1. Introduction

In modern high-performance turbo engines, the leakage losses generated from the rotor tip clearance flow (including the relative leakage flow rate and leakage flow loss) accounts for a sizeable proportion of the total losses in a turbine stage. For a long time, in order to reduce these losses, researchers have made painstaking efforts to explore a number of effective methods, and many of them have been applied to engineering practice. Among them, the curved and twisted blade technique has been proved to be an effective method. The mechanism of curved and twisted blade to reduce flow loss has been revealed in a turbine stator without clearance (Williams *et al.*, 2008; Liu T. and Woodiga, 2010). However, the mechanism of leakage losses under a different gap size and flow incidence angle is not identical. The mechanism of the curved blade to reduce leakage losses is not exactly the same.

Topological analysis is a theoretical tool to obtain the flow structure information from flow visualization pictures. It has been widely and successfully applied to the outflow research (Lighthill, 1963; Tobak and Peake, 1982; Liu M., 1987; Dellery, 1991; Bringhenti and Barbosa, 2008). Wang Zhongqi and his research group (Song, 1997; Su and Wang, 1992; Huang, 1997; Kang, 1990; Zhang, 2007; Yang, 2006) introduced the topology method to analyze the flow in turbo-machinery, derived the topology rules of annular rotor and stator both of the wall and

cross-section flow. Detailed analysis of wall and cross-section flow pictures in an annular compressor cascade with tip clearance was performed and provided the topology and vortex structure of this type of cascade. It pointed out that the concentrated shedding vortex plays a dominant role in the generation of flow losses.

On this basis, in this paper, the ink flow visualization method is adopted to study the flow patterns on both the blade surface and end wall in a turbine cascade with a gap of 0.036 span heights. By topology analysis, the topology and vortex structure under different incidence angles of the tested cascade is achieved, and then, the similarities and differences of the flow structure of incidence angle and stack line are discussed to reveal the mechanism of energy loss generation and the curved blade to reduce losses (especially leakage loss) in a turbine cascade with tip clearance.

2. Test models

A five-hole probe is used to measure the flow field parameters both in rectangular cascades and in tip clearance. The ink visualization is performed on the blade surface and end wall. The experiment is conducted by the low-speed cascade wind tunnel of Harbin Institute of Technology (shown in Fig. 1a). The air flow comes from a 75 kW centrifugal fan. The airflow is compressed by the centrifugal fan into a 3m long regulator tube, the honeycomb, convergence tube, inlet part, side plate, tested cascade and tailgate in turn. With the stepper motor and coordinate frame of the test system, the probes can move in three directions (x, y, z) and rotate around its own axis, which can measure the cascade along the axial, spanwise and pitchwise direction.

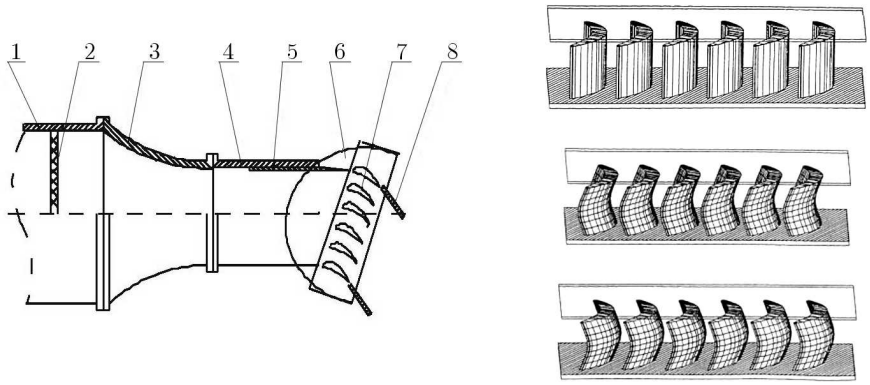

Fig. 1. Schematic of the low speed wind tunnel and tested cascade models; (a) low-speed cascade wind tunnel (1 – regulator tube, 2 – honeycomb, 3 – convergence tube, 4 – inlet part, 5 – side plate, 6 – rotating disc, 7 – tested cascade, 8 – tailgate), (b) tested cascades

The test models contain three sets of gas turbine rectangular cascades: conventional straight cascade; the 20° positive curved cascade; and the −20° negative curved cascade (shown in Fig. 1). The cascade parameters are shown in Table 1. In this paper, the ink display method is used to reveal the flow pattern through the topological vortex structure, and therefore, there is no further discussion on flow field measurement results.

In this study, the ink display method is used to show that the flow patterns both on the blade and end wall. First, we need to drop some ink droplets in the appropriate position of the blade surface. When the fan works properly, the air flow channel gate is opened to control the airflow flow rate. The ink droplets move along the blade surface and end wall with a certain speed of the airflow and drags a track which can be identified as the limiting streamlines on the surface. Through a combination of the flow parameters measured by probes and the topological analysis, we can get the detailed flow structure of the cascade flow.

Table 1. Geometry data of the tested cascades

Blade chord	$b = 120.5\,\text{mm}$	Outlet metal angle	$\alpha_{2p} = -63^\circ$
Span	$h = 110\,\text{mm}$	Camber angle	$\Delta\alpha = 113^\circ$
Pitch	$t = 90\,\text{mm}$	Blade counts	$N = 6$
Relative chord length	$t/b = 0.763$	Tip clearance	$\tau = 4\,\text{mm}$
Axial chord	$B = 118.5\,\text{mm}$	Relative tip clearance	$\overline{\tau} = \tau/h = 0.036$
Aspect ratio	$h/b = 0.913$	Total pressure at inlet	$P_0^* = 10730\,\text{Pa}$
Leading edge radius	$R_1 = 6.75\,\text{mm}$	M at outlet mid-span	$M = 0.3$
Trailing edge radius	$R_2 = 3.37\,\text{mm}$	Re (based on chord)	$\text{Re} = 8.3 \cdot 10^5$
Inlet metal angle	$\alpha_{1p} = 50^\circ$	Inlet boundary layer thickness	$\delta = 14\,\text{mm}$

3. Topology rules

The surfaces of a cascade with tip clearance can be decomposed into two unconnected surfaces: casing and rotor surface. In which, the rotor surface contains of the blade surface and hub. The friction lines are surrounded with many odd points on these surfaces.

On the surface, the three-dimensional separation of the Lighthill model gives the total number of nodes, and the saddle points should satisfy the relationship below

$$\sum N - \sum S = 2(2 - n) \tag{3.1}$$

Among them, n is the number of connected domains and N and S, respectively, for the number of nodes and saddle points. For the annular cascade with tip clearance, the blade surface and the inner ring form a connected domain while the outer ring forms another one. Thus, the odd points on the blade surface and hub wall should follow the following equation

$$\sum N_{bh} - \sum S_{bh} = 0 \tag{3.2}$$

where $\sum N_{bh}$ and $\sum S_{bh}$ represents the total number of nodes and saddle points on the blade surface and hub wall.

The flow on the shroud wall is governed by the same topological rules

$$\sum N_c - \sum S_c = 0 \tag{3.3}$$

where $\sum N_c$ and $\sum S_c$ represents the total number of nodes and saddle points on the shroud wall.

The flow patterns around the solid cascade surface with tip clearance, on the whole, have the same numbers of node and saddle points. The topologies of rectangular cascades with tip clearance equivalents to that of annular cascades and follow the topological rules above.

4. Topology and vortex structure under zero incidence angle

4.1. Topology analysis of straight cascades shroud with tip clearance

Figures 2a-c illustrates the ink visualizations on the shroud wall of the straight, positive curved and negative curved cascades. Figure 2d gives out the topology structures. The figures show that the characteristics flow patterns at the shroud wall contains a double saddle point near the tip leading edge, the separation line Ls and the reattachment line Lr. Within one pitch on the shroud wall there are two areas, one is the tip clearance area, and another area is the

flow area. If it is bounded by the tip suction side, the transverse pressure gradient is opposite at these two sides. The end wall boundary layers clustered near the tip suction and pressure side or even separated under the effects of the pressure gradient and formed a separation line Ls and a reattachment line Lr. Along the pitchwise direction, the static pressure on Ls are minimum, the limiting streamlines asymptotic to it on both sides, the separation line starting from Ls and flows into the far field. The static pressure on Lr are maximum, the limiting streamlines depart from it on both sides, which means that the far field flows toward the end wall.

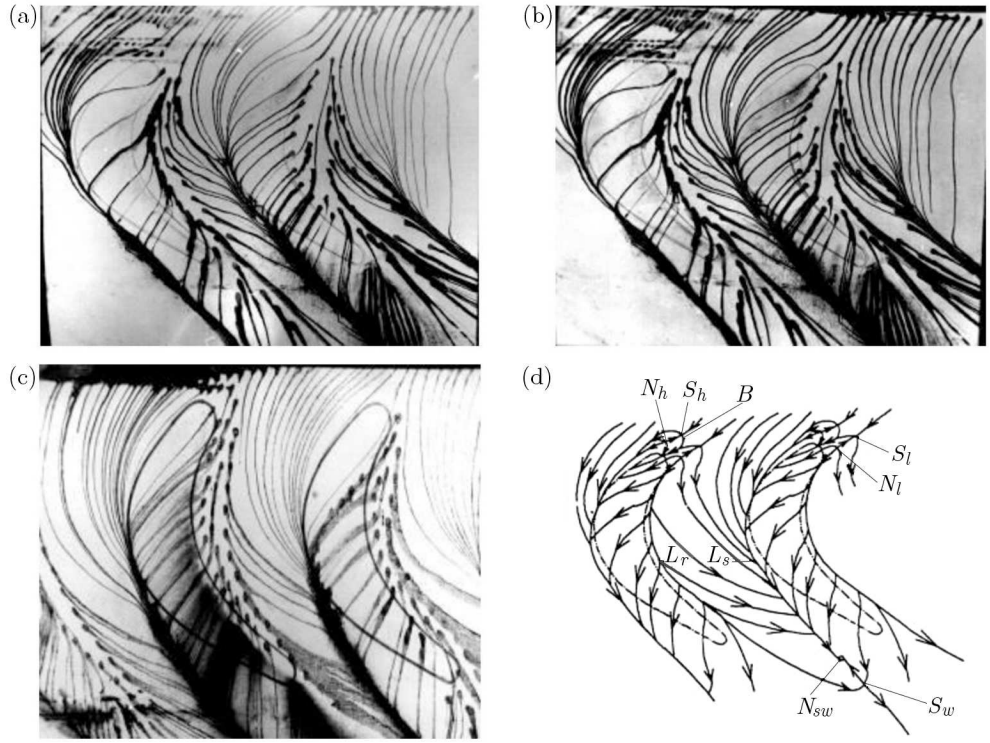

Fig. 2. Flow visualization on the tip wall (incidence 0°); (a) straight cascades, (b) positive curved cascades, (c) negative curved cascades, (d) topology structure at clearance

The transverse pressure gradient within the flow and gap will affect the circumferential distribution of static pressure in the upper region of the leading edge. The kind of topological structure on the leading edge end wall is closely related to the circumferential distribution of local static pressure.

At the side without clearance, the transverse pressure gradient only has one direction within one pitch. In this casing, it forms a single saddle point separation. At the side with clearance, affected by the transverse pressure gradients which have the opposite direction in the flow passage and tip clearance, there occur two areas with the opposite pressure gradient in front of the leading edge. Under the action of the opposite direction pressure gradient within the end wall boundary layer, there forms a special flow pattern with two saddle points (S_h, S_l) and two nodes (N_h, N_l) on the suction side and pressure side of the leading edge. As Fig. 2d shows, the friction lines through the saddle point S_h on the suction side of the leading edge have two branches. It indicates that if there is a tip clearance, partial flow of the inlet end wall boundary layer forms the suction side horseshoe vortex in front of the leading edge. Among them, the suction side branches around the leading edge enter into the suction side of the shroud corner under transverse pressure gradient and join with the leakage vortex separation line Ls at about 0.05 axial chord locations. The pressure side branches flow downstream and enter into the tip clearance. Under the same transverse pressure gradient, it slants through the tip and merges with the leakage vortex separation line Ls at about 0.25 axial chord locations. In

area B, where these two branches surrounded, the limiting streamlines gradually move closer to these two branches and form an attached node point N_h at the downstream of S_h. This flow phenomenon also occurs on the pressure side. Another part of the inlet end wall boundary layer separates from the saddle point S_l and forms the pressure side of the horseshoe vortex. The suction side branches flow downstream and meet with the pressure side separation lines of the suction side horseshoe vortex. The pressure side branches slant through the flow passage and converge to the separation line Ls under the transverse pressure gradient and form an attached node point N_l at the downstream of S_l. As the separation line Ls and the reattached line Lr stretch downstream, these two lines intersect at about 1/3 axial chord beyond the trailing edge and form a saddle point S_w. One of the separation lines started from S_w extends further to the downstream, and the other one moves upstream into the spiral point N_{sw}.

On the whole, there are three saddle points, two reattached node points and one separation spiral point on the shroud wall with tip clearance. Total number of singular points follows the topology rules shown in Eq. (3.2).

4.2. Topology analysis of straight cascades blade and hub with tip clearance

Figure 3 shows the ink track and topological structure on the blade surface and the end wall of the straight cascades. During the ink trace test, the development of the ink trace is recorded instantly to describe the specific topological disciplines. It can be seen that the reattachment line started from the attached node point N_{am} near the leading edge middle span climbs towards upper blade span and gets into the tip clearance with leakage flow. The reattachment line diagonally crosses the blade tip and intersects the blade tip suction side at about 30% axial chord length. And then it enters the extension below the suction side and inclined slightly to form a saddle point S_c. From the saddle point, there are two separation lines. One of them develops along the tip suction side to the downstream and ends in the separation point N_{st} near the trailing edge. Another one extends into the bottom of the suction side and gets into the separation point N_{su} at 1/3 span height away from the tip. The attached node point N_c is formed at downstream of S_c. There are two reattachment lines from N_c. One of them reversely flows upstream S_c, and the other one flows downstream and meets the trailing edge at about 1/5 span from the tip and forms the saddle point S_u. In the picture, we also could find separation in the tip clearance flow. There are two separation lines from the saddle point S_d at about 35% axial chord. One of them meets the separation branches of S_c along the blade tip suction side, and another one overlaps with the edge of blade tip pressure side and ends on the pressure side trailing edge separation node N_{pt}. At the downstream of S_d, there forms an attached node point N_d.

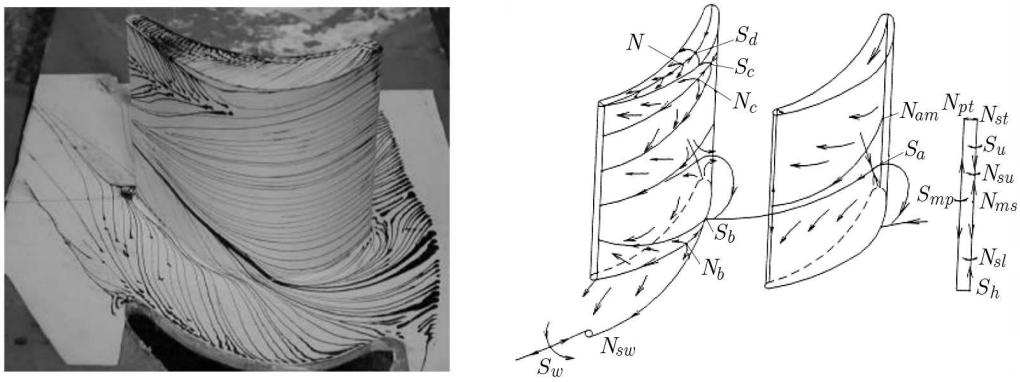

Fig. 3. Ink track and topological structure on the blade surface and the end wall of straight cascades (incidence 0°)

The similar flow conditions occurs in the lower end wall and suction surface comparing to the flow within no-gap cascade. The end wall boundary layer meets the cylindrical inlet edge and forms a separation saddle point S_a and two horseshoe vortex branches. The pressure branch diagonally crosses the flow channel and meets the horseshoe vortex suction side branch of the adjacent blade passage and forms the saddle point S_b. One of the separation lines ends in the separation node point N_{Sl}, and another one ends in N_{sw}. There is a saddle point S_w. One of the two separation lines ends in N_{sw}, and the other flows downstream. The reattachment lines from N_b also end in S_h.

The tip clearance leakage flow starts from the pressure side to the suction side and the cross flow at the bottom end wall is also from the pressure side to the suction side. Therefore, the limiting streamlines of the pressure surface extend to both end walls form the middle span. It forms a reattached line from N_{am} which ends in S_{mp}.

In the conventional straight cascade, there have nine saddle points, four attached points, four separation points and a separation spiral point. The total number of singular points follows Eq. (3.3).

4.3. Impact of curved blade on topology and vortex structure

Figures 4a,b show the ink track of positively and negatively curved cascades. Compared with the straight cascades, the topological and vortex structure of negative curved cascades is similar to it, while the positive curved cascades are different. The negative curved cascades only change the position of singular points, while remain its type and numbers unchanged. As the ink track shows, the positive curved cascades eliminate the separation line of the upper passage vortex and the numbers of singular points thus is reduced from 24 (total number of Fig. 2d and Fig. 4) to 20 (total number of Fig. 2d and Fig. 6).

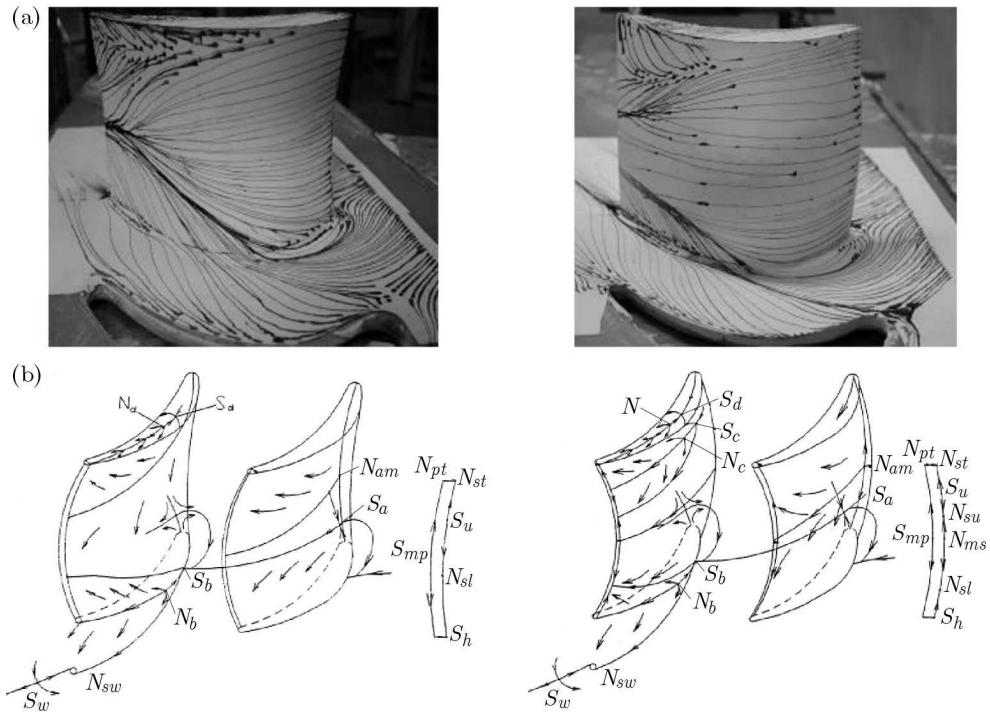

Fig. 4. Ink track and topological structure on the blade surface and the end wall of positive and negative curved cascades (incidence 0°); (a) ink track visualization (left – straight cascades, right – positive curved cascades), (b) topology structure (left – positively curved cascades, right – negatively curved cascades

The positive curved cascades change the topology structure and improve the aerodynamic characteristics of the cascade are because:

1) the positive curved cascades reduce the singular and semi-odd points and also reduce the viscous shear effects and entropy increase;

2) it eliminates the upper passage vortex and prevents the cross flow to be pushed to the middle span but attaches to the upper end wall and enhances the block of leak flow;

3) positive curved cascades reduce the pressure difference between the tip pressure side and suction side, weaken the driving force of the leakage flow.

As for the negative curved cascades, the impact on leakage flow rate is just opposite. The anti-C-type of pressure contours pushes the upper passage vortex to the tip region and enhances the block of leakage flow. The enhanced pressure difference between the pressure side and suction side strengthens the driving force of the leakage flow. Compared with the straight cascades, the increase or decrease of leakage flow rate depends on which aspect is dominant. While the tip clearance is 0.036, the pressure difference plays the main role and thus the leakage flow rate in negative curved cascades is larger.

5. Topology and vortex structure under 20° incidence angle

Figure 5 shows the ink track of these three sets of cascades at 20° incidence angle. Compared with Fig. 2, in addition to the location of the singular points and separation range, these three sets of cascades have the same number and type of singular points. At 20° incidence angle, the

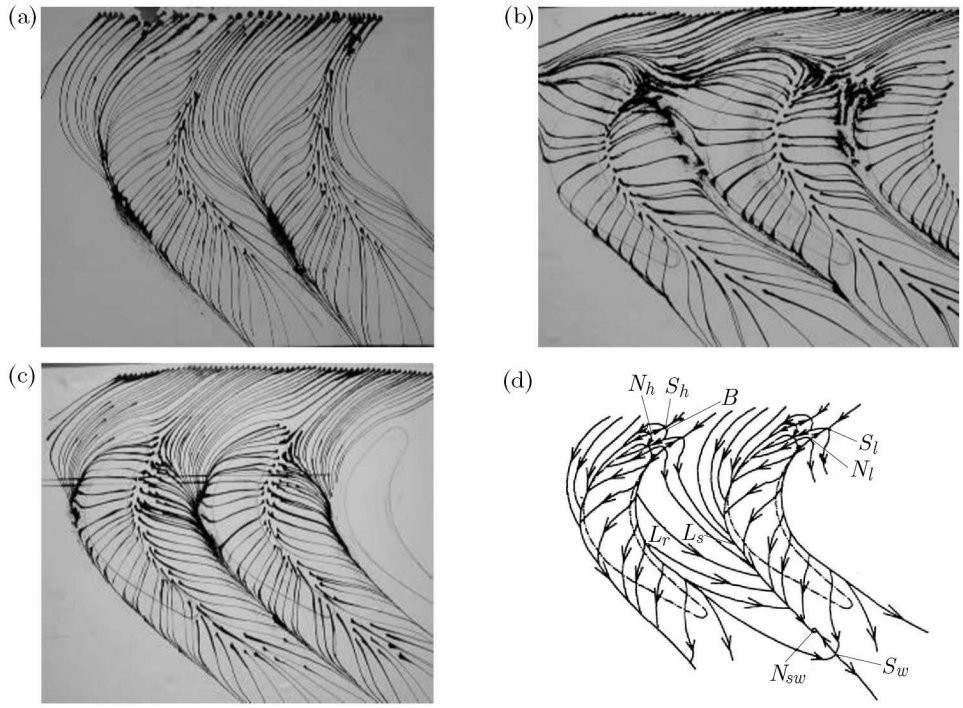

Fig. 5. Flow visualization on the tip wall (incidence 20°); (a) straight cascades, (b) positive curved cascades, (c) negative curved cascades, (d) topology structure at clearance

saddle points S_l and S_h move to the upstream and middle passage. The region surrounded by the two branches of the horseshoe vortex extends along the flow direction. The meeting location of these two separation lines with L_s moves upstream. The limiting streamlines tend to be

perpendicular to the pressure and suction sides. The changes of upper end wall topology are all because the leading edge blunting and cross pressure gradient increase with the increase of the flow attack angle.

Figures 6 and 7 illustrate the ink visualizations on the shroud wall of the straight, positive curved and negative curved cascades at 20° incidence angle and 0.036 relative tip clearances. Compared to Fig. 2, the main changes are: first, S_a, the saddle of the leading edge at the lower endwall of the blade moves to the upstream and the middle passage of the cascade. S_b, S_c and S_α, which represent the saddle point near the suction side at the lower endwall, the saddle point near the suction side, and the saddle point on the blade tip, also move upstream. This shows that the horseshoe vortex of lower end wall, the upper and lower passage vortex, the suction side corner vortex, the tip separation vortex and the secondary vortexes occurred in the more upstream location, the vortex intensity are increased at the same axial chord position. Secondly, the separation lines of the lower and upper passage vortex meet at about 75% of the axial chord from the leading edge, these two contrary rotated passage vortexes converge at this location and exhibit intense interaction, and the eddy dissipation loss rapidly increases. It can be inferred that within the straight cascade flow loss, the passage vortex and tip leakage vortex interaction loss accounts for a major proportion at the zero attack angle while the lower and upper passage vortex convergence loss accounts for the main part at 20° incidence angle. Thirdly, because the separation lines of the upper and lower passage vortex meet together, the total number of singular points of the straight cascade reduce from 18 to 16, including one saddle point and one separation node.

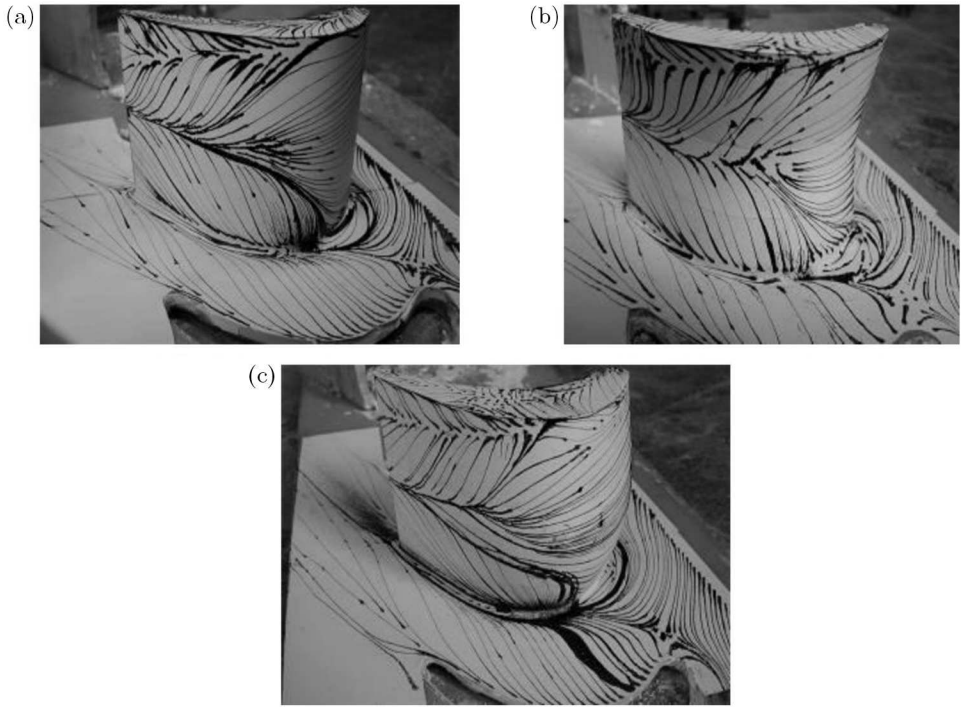

Fig. 6. Flow visualization on the end wall and blade surface of the three cascades (incidence 20°); (a) straight cascades, (b) positive curved cascades, (c) negative curved cascades

The number and type of singular points on the blade surface and the lower end wall of positive curved cascades are the same both at zero and 20° incidence angles. The saddle point S_a and S_b locate in the most upstream position as well as the horseshoe vortex and lower passage vortex. The lower passage vortex climbs up to the middle span at about 30% of the axial chord and moves downstream. As decried above, the positive curved cascade eliminates the upper passage vortex, there does not exist a counter rotating vortex at the middle span.

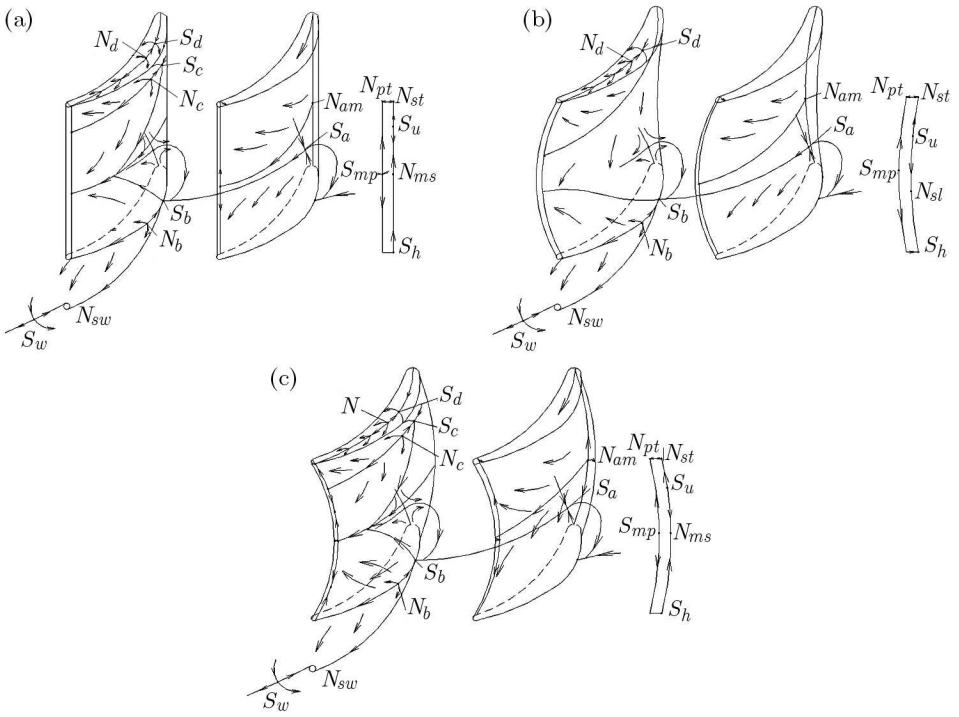

Fig. 7. Topology and vortex structure on the end wall and blade surface of the three cascades (incidence 20°); (a) straight cascades, (b) positive curved cascades, (c) negative curved cascades

Compared to that at zero incidence angles, the positive incidence angle does not bring a greater loss. It means that the positive curved cascades reduce the flow loss more significantly than zero incidence situations.

The number and type of the singular point on the blade surface and lower end wall of negative curved cascades are the same both at the zero and 20° incidence angle, only the locations change. The four saddle points (S_a, S_b, S_c and S_α) locate more upstream than the zero incidence situations and more downstream than 20° incidence angle situations of straight cascades. The lower and upper passage vortexes meet with each other at the upstream of trailing edge.

6. Conclusions

Through ink visualizations and topology analysis of the flow in different cascades, this article establishes the topology and vortex structures in a bent cascade with large tip clearance. From the point of view of identification of the fine structure of the flow field, it has been revealed that the blade bent led to a relative increase or decrease in the amount of the leakage flow rate and loss mechanism. It comes to the following conclusions:

- The positive curved blade cascade with tip clearance leads to significant changing of the topology and vortex structure under zero incidences. One is to reduce the number of singular points and half ones, and reduces the entropy increase of flow around the cascades as well as the viscous shear wall effects; the second is to eliminate the upper passage vortex and reinforce leakage flow cross-blocking force caused by the end wall cross flows. The negative curved blade cascade only changes the location of singular points and remains the type and numbers unchanged. The improvements of aerodynamic performance by the negative curved cascade are lower than those of positive ones.

- The total number of singular points on the wall surface of straight cascades decrease when the flow incidence angle increases from 0° to 20°. Compared with the zero incidence cases, the saddle points of the three sets of cascades move forward, the scope of the separation region expands along the flow and vertical direction and the separation lines of the lower and upper passage vortex climbs to the middle span. In the straight cascade, these two separation lines meet at about 75% of the relative chord at the middle span. The lower and upper passage vortexes with the opposite rotary direction mix and increase the flow loss. The positive curved cascade also eliminates the upper passage vortex and reduces the extra loss caused by the lower and upper passage vortex mixing. The separation lines of the lower and upper passage vortex in the negative curved cascade meet later along the flow direction than that in the straight cascade.

Acknowledgements

This work was supported by the National Natural Science Founding of PR China under Grant No. 51121004.

References

1. Bringhenti C., Barbosa J.R., 2008, Effects of turbine tip clearance on gas turbine performance, *Proceedings of ASME GT2008*, GT2008-50196
2. Dellery J., 1991, *Physique des Ecoulements Tourbillonnaires*, AGARD CP-494
3. Huang H., 1997, *Effect of Blade Curving on Flow and Vortex Structure in Cascades with Tip Clearance and a Simple Model for Predicting Losses in Curved Blade Cascades*, Doctoral dissertation of Harbin Institute of Technology
4. Kang S., 1990, An application of topological analysis to study the three-dimensional flow in cascades: part I-topological rules for skin-friction lines and streamlines,*Applied Math. And Mechanics*, **11**, 5, 489-495
5. Lighthill M.J., 1963, *Attachment and Separation in Three-Dimension Flow*, Oxford University Press
6. Liu M., 1987, Application of critical point theory, topology and bifurcation theory to separation and vortex flows, *Lecture Notes given at University of Tennessee Space Institute and New York Polytechnic University*
7. Liu T., Woodiga S.A., 2010, Experimental examination of skin friction topology in separated flows, *48th AIAA Aerospace Sciences Meeting*, AIAA-2010-0045
8. Song Y., 1997, *An Experimental Investigation into the Influence of the Blade Curving on the Flow Field Structure and Performance in an Annular Turbine Cascade*, Doctoral dissertation of Harbin Institute of Technology
9. Su J., Wang Z., 1992, Profiling of simultaneously vaulted and twisted blades-theory, experiment, design and application, *Power Engineering*, **12**, 6, 1-6
10. Tobak M., Peake D. J., 1982, Topology of three-dimensional separation flows, *Annual Review of Fluid Mechanics*, **14**, 1, 61-85
11. Williams R., Gregory S.D., He L., 2008, Experiments and computations on large tip clearance effects in a linear cascade, *Proceedings of ASME GT2008*, GT2008-50557
12. Yang Q., 2006, *Experimental Investigation of the Effect of Tip Clearance Size and Incidence on Turbine Cascade Flow Filed Structure*, Doctoral dissertation of Harbin Institute of Technology
13. Zhang H., 2007, *Investigation on Application of Dihedral/Swept Blade and Boundary Layer Suction to Control Vortex Configurations in Compressor Cascades*, Doctoral dissertation of Harbin Institute of Technology

Badania topologii i struktury wirów palisady turbiny z luzem wierzchołkowym przy różnych kątach natarcia

Streszczenie

W pracy zaprezentowano wyniki pomiarów eksperymentalnych trzech zestawów konwencjonalnych palisad turbin o prostym, dodatnio i ujemnie zakrzywionym profilu. Zbadano wpływ kąta natarcia oraz efekt zginania łopatek na straty wskutek upływu przy luzie wierzchołkowym sięgającym 3.6% rozpiętości łopatek. Do analizy zastosowano wizualizację śladów pozostawianych barwnikiem oraz teorię topologii, tj. struktur topologicznych reprezentujących powierzchnię łopatki oraz górnej i dolnej ściany krańcowej. Zaobserwowano, że w porównaniu do analogicznej palisady o zerowym kącie natarcia wszystkie punkty siodłowe przesuwają się w górę przepływu, a obszar oderwania strugi rozszerza się wzdłuż promienia łopatki. Jednocześnie granica oderwania górnego i dolnego wiru przemieszcza się ku środkowi łopatki, gdy kąt natarcia narasta od zera do 20°. Przy tych granicznych wartościach kąta natarcia łopatki o dodatniej krzywiźnie profilu eliminują górny wir podczas przejścia. Ponadto okazało się, że liczba punktów osobliwych zmniejszyła się podobnie, jak osłabiła się interakcja pomiędzy wirami przejścia i wirami upływu. Stwierdzono, że wzmacnia to efekt blokowania upływu poprzecznym przepływem na krańcowej ścianie łopatki, co ostatecznie redukuje straty indukowane upływem.

Manuscript received May 8, 2012; accepted for print June 24, 2012